

Domain State of the ANNNI model in Two Dimensions

Fumitaka Matsubara

Department of Applied Physics, Tohoku University, Sendai 980-8579, Japan

Takayuki Shirakura*

Faculty of Humanities and Social Sciences, Iwate University, Morioka 020-8550, Japan

Nobuo Suzuki

Faculty of Science and Technology, Tohoku Bunka Gakuen University, Sendai 980-8551, Japan

(Dated: October 9, 2018)

We have examined the spin ordering of an axial next-nearest-neighbor Ising (ANNNI) model in two dimensions (2D) near above the antiphase ($\langle 2 \rangle$ phase). We considered an N_R -replica system and calculated an overlap function q_m between different replicas having used a cluster heat bath (CHB) Monte Carlo method. We determined transition temperature between $\langle 2 \rangle$ phase and a floating incommensurate (IC) phase as $T_{C2}/J = 0.89 \pm 0.01$ with frustration ratio $\kappa (\equiv -J_2/J_1) = 0.6$. We found that the spin state at $T \gtrsim T_{C2}$ may be called as a domain state, because the spin structure is characterized by a sequentially arranged four types of domains with different $\langle 2 \rangle$ structures. In the domain state, the 2D XY symmetry of the spin correlation in the IC phase weakly breaks and the diversity of the spin arrangement increases as $T \rightarrow T_{C2}$. The Binder ratio g_L exhibits a depression at $T \sim T_{C2}$ and the quasi-periodic spin structure, which is realized in the IC phase, becomes diverse at $T \gtrsim T_{C2}$. We discussed that the domain state is stable against the thermal fluctuation which brings a two-stage development of the spin structure at low temperatures.

I. INTRODUCTION

Systems with competitive interactions have been extensively studied throughout the past three decades, because they exhibit rich physical phenomena, such as commensurate-incommensurate phase transitions, Lifshitz points and multiphase points.¹ The axial next-nearest-neighbor Ising (ANNNI) model is among the simplest realizations of such systems. In the two-dimensional (2D) ANNNI model, ferromagnetic Ising chains are coupled by ferromagnetic nearest-neighbor and antiferromagnetic next-nearest-neighbor interchain interactions on a square lattice. The Hamiltonian is described by

$$\mathcal{H} = -J \sum_{x,y} S_{x,y} S_{x+1,y} - J_1 \sum_{x,y} S_{x,y} S_{x,y+1} - J_2 \sum_{x,y} S_{x,y} S_{x,y+2}, \quad (1)$$

where $S_{x,y} = \pm 1$ is an Ising spin. In this paper we consider the case with $J_1 = J > 0$ and $J_2 < 0$. The ground state of the model is a ferromagnetic long range order (LRO) phase for frustration coefficient $\kappa (\equiv -J_2/J) < 1/2$ and a LRO antiphase ($\langle 2 \rangle$ phase) for $\kappa > 1/2$, in which the $\langle 2 \rangle$ phase is described by an alternate arrangement of two up-spin and two down-spin chains in the y -direction. This model at finite temperatures has been studied throughout the past few decades by various methods.²⁻⁷ It was suggested that, for $\kappa > 1/2$, a floating incommensurate (IC) phase exists between the $\langle 2 \rangle$ phase and the paramagnetic (PM) phase.^{2,3} The IC phase close to the higher transition temperature, T_{C1} , may be characterized by dislocations³ that play the same role of vortices in two-dimensional XY (2D XY) model,⁸ and the

IC phase near above the lower transition temperature, T_{C2} , may be characterized by domain walls of three up-spin chains or three down-spin chains penetrating the $\langle 2 \rangle$ phase. However, the spin ordering is yet to be clarified, because recent Monte Carlo (MC) studies predicted different spin orderings. While equilibrium MC simulations supported the above picture of the spin ordering with $T_{C2} < T_{C1}$,^{9,10} a nonequilibrium relaxation (NER) MC method^{11,12} predicted $T_{C2} \sim T_{C1}$, i.e., the absence of the IC phase.^{13,14} In a previous paper¹⁵ (referred as I, hereafter), we reexamined the spin ordering of the ANNNI model with $\kappa = 0.6$ near T_{C1} having used both the equilibrium MC and the NER MC methods and showed that both methods give almost the same transition temperature of $T_{C1} \sim 1.16J$ and the spin ordering at $T \lesssim T_{C1}$ exhibits properties of the 2D XY model.⁸

In this paper, we reexamine the spin ordering near the other transition temperature T_{C2} . We will propose a physical quantity appropriate for the ANNNI model, by which we can readily separate $\langle 2 \rangle$ phase from the IC phase. Section II describes the investigated method and quantities of the 2D ANNNI model. Section III presents results of the equilibrium simulation. In Sec. IV, we discuss, on the basis of a domain picture, the spin structure of the model for both the temperature ranges of near below T_{C1} ($T \lesssim T_{C1}$) and near above T_{C2} ($T \gtrsim T_{C2}$). Section V is addressed on the periodic nature of the ANNNI model calculating the Fourier component of the spin arrangement. Section VI is devoted to conclusions and discussions, where we will discuss why the 2D ANNNI model undergoes a very slow relaxation at low temperatures.

II. METHOD AND QUANTITIES

We apply a similar technique as proposed by Sato and Matsubara(SM)⁹ and used in I. We consider the model with $\kappa = 0.6$ on the $L_0 \times L_0$ lattice with open boundaries. Quantities of interest are measured in the inner region of $L \times L$ with $L = L_0/2$, i.e., $L_0/4+1 \leq x, y \leq 3L_0/4$. Hereafter we attach a new lattice site name for this region, i.e., $x, y = 1, 2, \dots, L$. We apply the CHB algorithm^{16,17} to get an equilibrium spin configuration. That is, the spin configuration of a block of $L_0 \times l_y$ spins is updated using the transfer matrix method, where the transfer direction is the x -direction (L_0) and the width of the block l_y is determined from the computational time costs. In the previous paper we apply the SM procedure with $l_y = 6$. The choice of $l_y = 6$ was appropriate in a temperature range of $T \sim T_{C1}$. However, when the temperature is lowered toward T_{C2} , the number of the MC sweeps needed to get the equilibrium spin configuration rapidly increases. Then we adopt a larger l_y for a larger lattice of $L_0 \times L_0$.

The difficulty of studying the phase transition of the ANNNI model is that the spin structure of the IC phase is not known a priori. Another problem to be noted is that the $\langle 2 \rangle$ phase has equivalent four structures. That is, when we look at four spins at $(4l + 1, 4l + 2, 4l + 3, 4l + 4)$ ($l = 0, 1, 2, \dots$) chains, they have either $(+ + - -)$, $(+ - - +)$, $(- - + +)$ or $(- + + -)$. One usually investigates the squared chain magnetization $M_2 (= \frac{1}{L} \sum_{y=1}^L (\frac{1}{L} \sum_{x=1}^L S_{x,y})^2)$. This quantity characterizes the spin correlation along the x -direction. Using M_2 , one can separate the IC phase from the PM phase, because in the PM phase M_2 exponentially decays with increasing L and M_2 will algebraically decays in the IC phase. However, near the lower transition temperature T_{C2} , calculation of equilibrium value of M_2 for a larger size L_0 is hard task^{9,15} and one searches for T_{C2} using different quantities.^{9,13} Moreover we can hardly investigate the 2D nature of the ANNNI model, in particular the spin correlation along the y -direction.

Here we consider another quantity for examining the 2D spin structure itself. We obtain the equilibrium spin configuration $\{S_{x,y}^0\}$ at a temperature T . That is, we get $\{S_{x,y}^0\}$ performing the MC simulation using some sequence of random numbers. Then, make the MC simulation at the same temperature T using a different sequence of random numbers and get the spin configuration $\{S_{x,y}\}$. We extract the $\{S_{x,y}^0\}$ component of $\{S_{x,y}\}$ by calculating the spin overlap between them. To realize this procedure, we consider an N_R -replica system. The spin configurations $\{S_{x,y}^\alpha\}$ ($\alpha = 1, 2, \dots, N_R$) of these replicas are generated by different sequences of random numbers. We define the \vec{k} -dependent maximum spin overlap function $q_m^{\alpha,\beta}(\vec{k})$ of the replica α and the replica β as

$$q_m^{\alpha,\beta}(\vec{k}) = q^{\alpha,\beta}(y_0, \vec{k}), \quad (2)$$

where

$$y_0 = \arg \max_{-L/2 \leq y' \leq L/2} q^{\alpha,\beta}(y', \vec{k}), \quad (3)$$

$$q^{\alpha,\beta}(y', \vec{k}) = \frac{1}{L^2} \left| \sum_{x=1}^L \sum_{y=1}^L S_{x,y}^\alpha S_{x,y+y_0}^\beta \exp(i\vec{k}\vec{r}_{x,y+y'}) \right|. \quad (4)$$

In the IC phase a drift of the spin configuration inevitably occurs along the y -direction. We take into account the drift by a uniform shift of the spin configuration y_0 . Also $q_m^{\alpha,\beta}(\vec{k})$ is free from the structure of the $\langle 2 \rangle$ phase. The overlap function $q_m(\vec{k})$ of the system is the average of those overlap functions.

$$q_m(\vec{k}) = \frac{2}{N_R(N_R - 1)} \sum_{\alpha \neq \beta} q_m^{\alpha,\beta}(\vec{k}) \quad (5)$$

Note that the overlap function at $\vec{k} = 0$, $q_m(\equiv q_m(0))$, plays the role of the order parameter of the ANNNI model. If q_m decays algebraically with increasing N , it reveals that the system is in the critical phase, i.e., the IC phase, while q_m remains non-zero constant, it reveals that the system is in the LRO phase, i.e., the $\langle 2 \rangle$ phase. In contrast, $q_m(\vec{k})$ for $\vec{k} \neq 0$ will be used to obtain the correlation length of the spin structure.

III. RESULTS

We investigate the equilibrium properties of the ANNNI model by the overlap function q_m . We focus our effort in the temperature range of $T \leq T_{C1}$ ($\sim 1.16J$). We perform the CHB simulation of the ANNNI model on lattices with $L_0 = 24 \sim 128$. We make two simulations: a gradual cooling simulation and a gradual heating simulation. In the gradual cooling (heating) simulation, we start with a PM ($\langle 2 \rangle$) spin configuration at a high (low) temperature and perform the simulation described below, then the temperature is lowered (raised) by some fixed interval ΔT and perform the same simulation starting with the last spin configuration at the previous temperature, and so on. For each temperature, after MCS_{equi} sweeps are discarded, data of interest are measured for every 10 sweeps over MCS_{mea} sweeps. Data presented here are averages of those of two simulations, and errors are differences between them. Hereafter averages of data Q in the inner $L \times L$ lattice are described as $\langle Q \rangle_L$. The parameters used in the equilibrium simulation are listed in Table I.

A. Spin overlap

Figure 1 shows $\langle q_m \rangle_L$ as functions of T for different L . At high temperatures, $\langle q_m \rangle_L$ for a larger L is smaller than that for a smaller L . As the temperature is decreased from a high temperature, $\langle q_m \rangle_L$'s for all L increase and come together at $T \sim 0.89J$. Below this temperature, the L -dependence of $\langle q_m \rangle_L$ is reversed. This result clearly reveals that some 2D LRO takes place at $T < 0.89J$. That is, the transition temperature between the IC phase

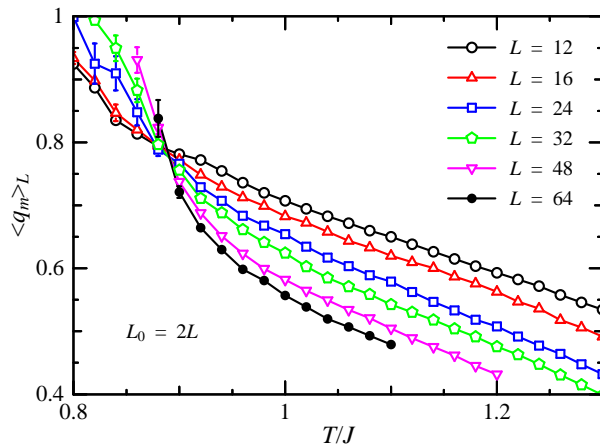


FIG. 1. (color online) Temperature dependences of the spin overlap function $\langle q_m \rangle_L$ in the ANNNI model with $\kappa = 0.6$, computed over the inner lattice with $L = L_0/2$.

and the $\langle 2 \rangle$ phase is $T_{C2}/J = 0.89 \pm 0.01$, because the LRO phase of the 2D ANNNI model is the $\langle 2 \rangle$ phase.

B. Binder Ratio

Next we consider the Binder ratio¹⁸ to examine the nature of the phase transition at T_{C2} . In a usual ferromagnetic(FM) model on a cubic lattice with the linear dimension L , the Binder ratio g_L of the magnetization M monotonically increases with decreasing temperature and reach 1 for $T \rightarrow 0$. In the PM phase, g_L decreases with increasing L , while g_L increases with L in the FM phase. Then the Binder ratio is independent of L at the critical temperature $T = T_C$. That is, the Binder ratios of different L 's intersect at $T = T_C$.

The Binder ratio g_L of q_m is defined as

$$g_L = \frac{1}{2} \left(3 - \frac{\langle q_m^4 \rangle_L}{\langle q_m^2 \rangle_L^2} \right). \quad (6)$$

Figure 2 shows temperature dependences of g_L for different L . They show unusual behaviors. For $T > T_{C2}$, g_L increases with L and seems to reach some finite value

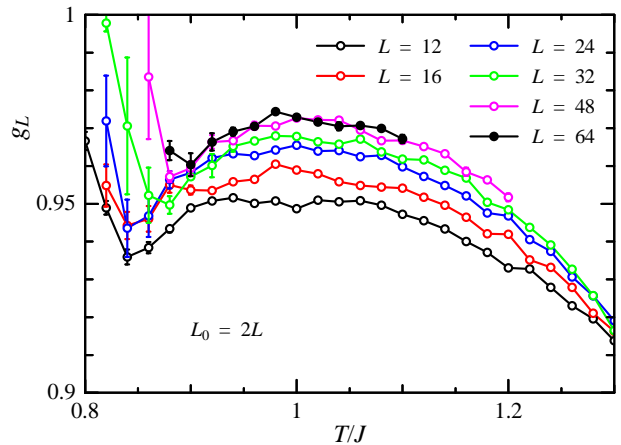


FIG. 2. (color online) Temperature dependences of Binder ratio g_L in the ANNNI model with $\kappa = 0.6$ and different L .

which is smaller than 1. On the other hand, for $T < T_{C2}$ g_L rapidly increases toward 1. This result is compatible with the fact that the IC phase for $T_{C2} < T < T_{C1}$ is the KT-like phase, i.e., a critical state, and that the $\langle 2 \rangle$ phase for $T < T_{C2}$ is the LRO phase. A queer point is its temperature dependence. As the temperature is decreased from a high temperature, g_L once increases, reaches its maximum value at $T \sim 1.00J$, then decreases down to around T_{C2} . That is, the phase transition at T_{C2} accompanies with a diversity of the spin structure.

We consider the distribution $P_L(q_m)$ of the order parameter q_m to investigate the diversity of the spin structure. Attention is paid whether $P_L(q_m)$ exhibits a usual single peak reminiscent of the continuous phase transition or a double peak of the first order phase transition. Figures 3(a)-(c) show $P_L(q_m)$ for $T \sim T_{C2}$. They exhibit a single peak revealing that the phase transition at T_{C2} is some continuous one. For $T > T_{C2}$, as L increases, the peak position $q_m^{(p)}$ shifts to the small q_m side and the peak height $P_L(q_m^{(p)})$ seems to saturate. These results are compatible with the L -dependences of $\langle q_m \rangle_L$ and g_L shown in Figs. 1 and 2, respectively. As $T \rightarrow T_{C2}$, $P_L(q_m)$ becomes broader and seems to be independent of L . For $T < T_{C2}$, the weight of $P_L(q_m)$ at smaller q_m diminishes and $P_L(1)$, which is the weight of the $\langle 2 \rangle$ phase, increases. Therefore the depression of g_L at $T \sim T_{C2}$ corresponds with a spread of $P_L(q_m)$. We believe the spread attributes to a characteristic nature intrinsic to the 2D ANNNI model. We consider the $\langle 2 \rangle$ phase with some $\langle 2 \rangle$ structures, i.e., a single-domain state $\{S_{x,y}^\alpha\}$. Suppose that one domain wall penetrates in the system. Then the system is separated into two domains with different $\langle 2 \rangle$ structures, i.e., a two-domain state $\{S_{x,y}^\beta\}$. The spin overlap function $q_m^{\alpha,\beta}(\vec{k})$ takes various values, depending on the location and the shape of the domain wall. Therefore the broad peak of $P_L(q_m)$ at $T \gtrsim T_{C2}$ may suggest that the system is composed of domains with

TABLE I. Parameters used in the CHB algorithm of the MC simulation of the $N_R = 8$ replica system. MCS_{equi} and MCS_{mea} are the number of MC sweeps required for equilibration and measurement, respectively.

L_0	l_y	MCS_{equi}	MCS_{mea}
≤ 48	6	4,000	12,000
64	8	10,000	30,000
96	10	20,000	60,000
128	12	40,000	80,000

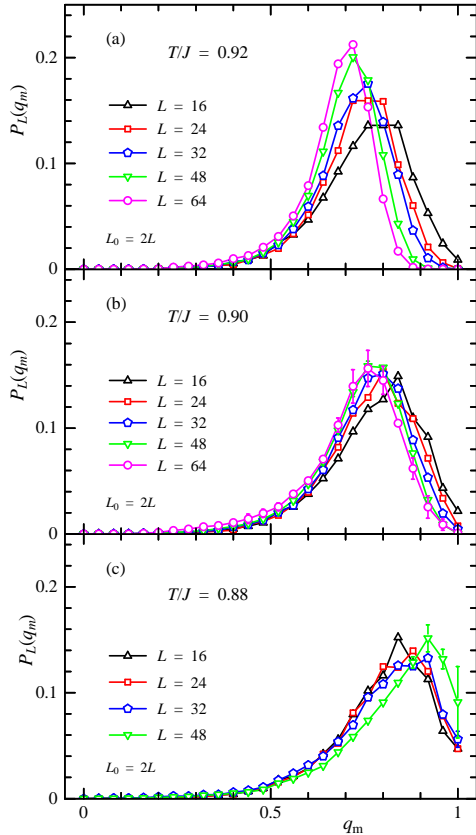


FIG. 3. (color online) Distribution $P_L(q_m)$ of the spin overlap q_m in the ANNNI model with $\kappa = 0.6$.

different $\langle 2 \rangle$ structures. In this temperature range, the spin correlations along the x - and y -directions will become anisotropic.

C. Correlation length

We consider the spin correlation length ξ_μ along the μ direction ($\mu = x, y$) to examine the speculation mentioned above. This quantity is obtained from the spin overlap function as follows:

$$\xi_\mu = \frac{1}{2 \sin(|\vec{k}_{\min}|/2)} \sqrt{\frac{\langle q_m^2 \rangle_L}{\langle |q(\vec{k}_{\min})|^2 \rangle_L} - 1} \quad (7)$$

where $\vec{k}_{\min} = (\pi/L, 0)$ and $\vec{k}_{\min} = (0, \pi/L)$ in the x and y direction, respectively. One usually studies the ratio of the correlation length ξ_μ to the linear lattice size L , ξ_μ/L , to determine the transition temperature T_C .¹⁹ Here we pay attention to the relation in the spin correlation between the x and y directions.

Figure 4 shows the correlation-length ratios ξ_x/L and ξ_y/L for different L as functions of T . In the x direction ξ_x/L smoothly increases with decreasing temperature. On the other hand, in the y direction ξ_y/L exhibits

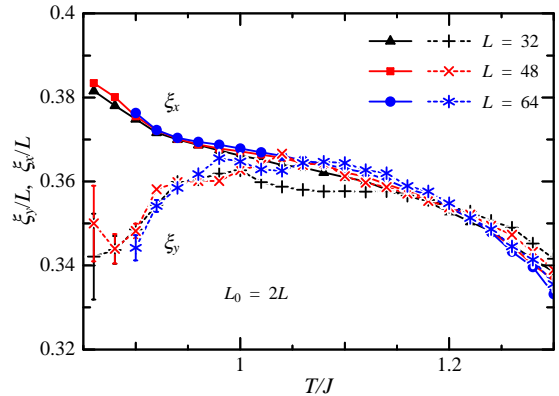


FIG. 4. (color online) Temperature dependences of the correlation-length ratios ξ_x/L (a) and ξ_y/L (b) in the x and y directions, respectively, in the ANNNI model with $\kappa = 0.6$.

an interesting behavior. As the temperature is decreased from a high temperature, ξ_y/L once increases, becomes maximum at $T \sim 1.00J$, then decreases down to T_{C2} . We note that the temperature dependence of ξ_y/L is quite similar to that of g_L shown in Fig. 2. This fact indicates that the diversity of the spin structure suggested by g_L and $P_L(q_m)$ comes from the decrease of the spin correlation along the y direction.

The remarkable point is that the nature of the spin correlation changes as the temperature is decreased toward T_{C2} . Of course, $\xi_y \sim \xi_x$ in the PM phase ($T > T_{C1} \sim 1.16J$). This relation holds near below T_{C1} and remains down to $T \sim 1.0J$. That is, for $T > 1.0J$ the system is almost isotropic for every direction like that of the KT phase in the 2D XY model. For $T \lesssim 1.0J$, ξ_x and ξ_y exhibit different temperature dependences, i.e., one increases with decreasing temperature and the other decreases. Therefore $T = 1.0J$ is a temperature below which the nature of the spin correlation gradually changes from that of the KT-like state to that of another state, probably a domain state.

IV. DOMAIN STRUCTURE

Now we examine the spin structure itself at $T \gtrsim T_{C2}$. Here we discuss it on the basis of the domain picture. For this aim, we define a domain valuable $\tau_{x,y}$ ($= a, b, \bar{a}$ or \bar{b}) which describes the element of the domain. Values of $\tau_{x,y}$ are determined as follows. We consider sequential four spins $(s_{x,y}, s_{x,y+1}, s_{x,y+2}, s_{x,y+3})$. Elements of the $\langle 2 \rangle$ structure are $(+1, +1, -1, -1)$, $(+1, -1, -1, +1)$, $(-1, -1, +1, +1)$, and $(-1, +1, +1, -1)$. These elements are distinguished by the location in the lattice. Since the $\langle 2 \rangle$ phase has the translational symmetry of $y \rightarrow y + 4l$ ($l = 1, 2, \dots$), if the spin arrangement of $(s_{x,y+4l}, s_{x,y+4l+1}, s_{x,y+4l+2}, s_{x,y+4l+3})$ is the same as

that of $(s_{x,y}, s_{x,y+1}, s_{x,y+2}, s_{x,y+3})$, $\tau_{x,y+4l} = \tau_{x,y}$. The spin configurations and domain values are listed in Table II. Hereafter we describe the domain composed of $d(= a, b, \bar{a}$ or $\bar{b})$ element as $D(= A, B, \bar{A}$ or $\bar{B})$ domain, respectively, and the domain wall between the D_1 and D_2 domains as $W_{D_1-D_2}$, where $D_1, D_2 = A, B, \bar{A}, \bar{B}$. When the D domain covers the whole lattice, we call the state the D-type $\langle 2 \rangle$ phase. We readily find an interesting property of the arrangement of neighboring two domains. If the domain wall is composed of three up-spin or down-spin chains, when we watch the domain with increasing the chain site y , the A follows the B , the B the \bar{A} , the \bar{A} the \bar{B} , and the \bar{B} the A . That is, the domains will appear sequentially as $A \rightarrow \bar{B} \rightarrow \bar{A} \rightarrow B \rightarrow A \rightarrow \bar{B} \dots$. An example of this is as follows.

y	1	2	3	4	5	6	7	8	9	10	11	12	
y_0	1	2	3	0	1	2	3	0	1	2	3	0	
$S_{x,y}$	+1	+1	-1	-1	+1	+1	+1	-1	-1	+1	+1	-1	
$\tau_{x,y}$	a	a	a	-	-	\bar{b}	\bar{b}	\bar{b}	\bar{b}	\bar{b}	-	-	
	13	14	15	16	17	18	19	20	21	22	23	24	25
	1	2	3	0	1	2	3	0	1	2	3	0	1
	-1	-1	+1	+1	-1	-1	+1	+1	+1	-1	-1	+1	+1
	\bar{a}	\bar{a}	\bar{a}	\bar{a}	\bar{a}	-	-	b	b	b	.	.	.

Figures 5(a) and (b) shows the snapshots of the domain structures at $T \lesssim T_{C1}$ and at $T \gtrsim T_{C2}$, respectively. For $T \lesssim T_{C1}$, the system is composed of small domains which are separated by tangled domain walls. On the other hand, for $T \gtrsim T_{C2}$, the system is composed of several large domains each of which runs across the lattice. That is, the difference in the domain structure between the two temperature ranges are the size of the domains. For either case, four types of the domains appear in order as speculated above. We calculate the average domain width W_L for different sizes L of the lattice and extrapolate it to $L \rightarrow \infty$. Figure 6 shows W_L as functions of T together with its extrapolation. As the temperature is decreased from a high temperature, W_L first increases slowly down to $T \sim 1.00J$, and then W_L increases rapidly and its extrapolation seems to diverge as $T \rightarrow T_{C2}$.

TABLE II. Spin arrangements of the domain element $\{S_{x,y}\} \equiv (s_{x,y}, s_{x,y+1}, s_{x,y+2}, s_{x,y+3})$ and the domain values $\tau_{x,y}(= a, b, \bar{a}$ or $\bar{b})$. Here the location of the element is distinguished by $y_0 = \text{mod}[y, 4]$.

$\{S_{x,y}\} \setminus y_0$	1	2	3	0
+1	a	\bar{b}	\bar{a}	b
+1	b	a	\bar{b}	\bar{a}
-1	\bar{a}	b	a	\bar{b}
-1	\bar{b}	\bar{a}	b	a

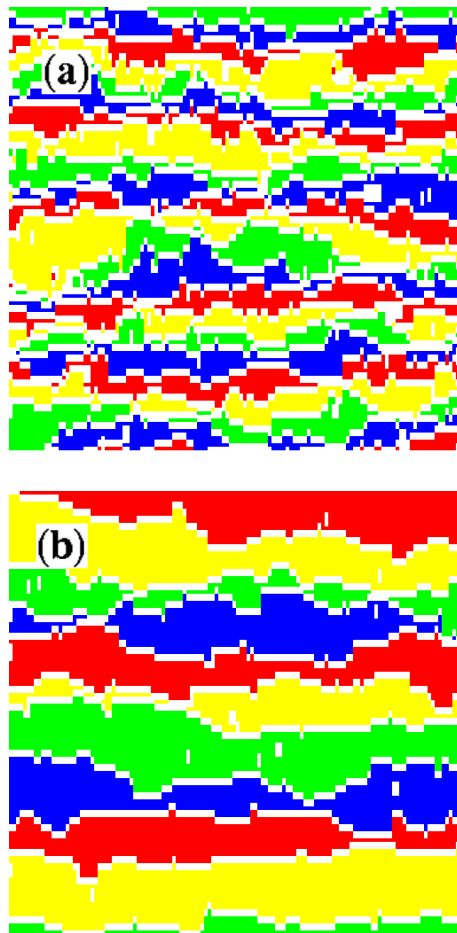


FIG. 5. (color online) Snapshots of the domain structure at (a) $T = 1.1J$ and (b) $T = 0.92J$ in the ANNNI model with $\kappa = 0.6$ on the 128×128 lattice. The domain elements a , b , \bar{a} , and \bar{b} are described by red, blue, green, and yellow, respectively, and the domain wall element by white.

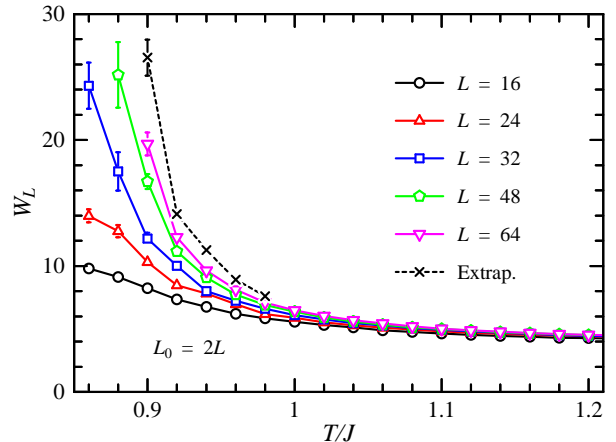


FIG. 6. (color online) Temperature dependences of the average domain width W_L of the lattice with L in the ANNNI model with $\kappa = 0.6$. The extrapolation to $L \rightarrow \infty$ is made using $W_L = W_\infty + A/L$ assumption.

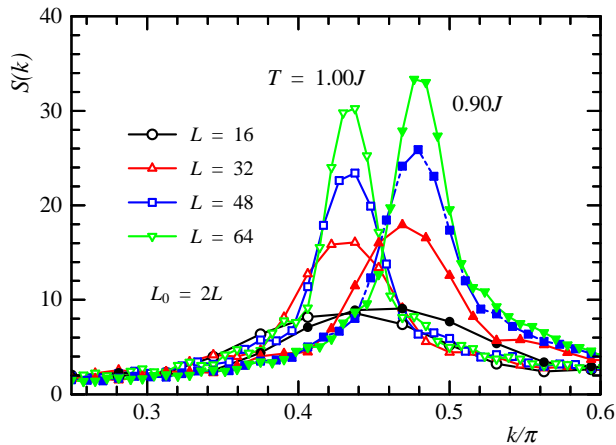


FIG. 7. (color online) The Fourier components of the spin structure $S(k)$ for two temperatures well-above (open symbols) and near-above (solid symbols) T_{C2} .

V. FOURIER COMPONENT $S(k)$

In an experimental point of view, the Fourier component of the spin arrangement is interesting. The Fourier component $S(k)$ along the y direction is given by

$$S(k) = \left| \sum_{y=1}^L m(y) \exp(iky) \right|, \quad (8)$$

where $m(y) (= \sum_{x=1}^L S_{x,y}/L)$ is the averaged magnetization of the y -th chain. This quantity gives the periodicity of the spin arrangement in the y direction. The period n of the spin arrangement is given by $n = 2\pi/k$ and the $\langle 2 \rangle$ phase corresponds to $k = \pi/2$. Figure 7 shows $S(k)$ at two temperatures of well-above and near-above T_{C2} for different size L . For either temperature, $S(k)$ exhibits a single rather broad peak which grows with increasing L . The result suggests that the system has a quasi-periodic spin arrangement characterized by the peak position $k^{(p)}$ and its deviation Δk . Note that the number of the periodic spin arrangements describing $S(k)$ is roughly given by $n_p \sim \Delta k / (\pi/L) = (\Delta k / \pi)L$. Thus Δk gives the diversity of the spin structure. Here we estimate the peak $k^{(p)}$ and its deviation Δk from

$$k^{(p)} = \frac{\sum_{k=\pi/L}^{\pi} k \tilde{S}(k)}{\sum_{k=\pi/L}^{\pi} \tilde{S}(k)} \quad (9)$$

$$(\Delta k)^2 = \frac{\sum_{k=\pi/L}^{\pi} (k - k^{(p)})^2 \tilde{S}(k)}{\sum_{k=\pi/L}^{\pi} \tilde{S}(k)}. \quad (10)$$

where $\tilde{S}(k) = S(k) - \sum_{k=\pi/L}^{\pi} S(k)/L$. We calculate $k^{(p)}$ and Δk for different L and extrapolate them to $L \rightarrow \infty$. Figures 8(a) and (b) show $k^{(p)}$ and Δk for different L as

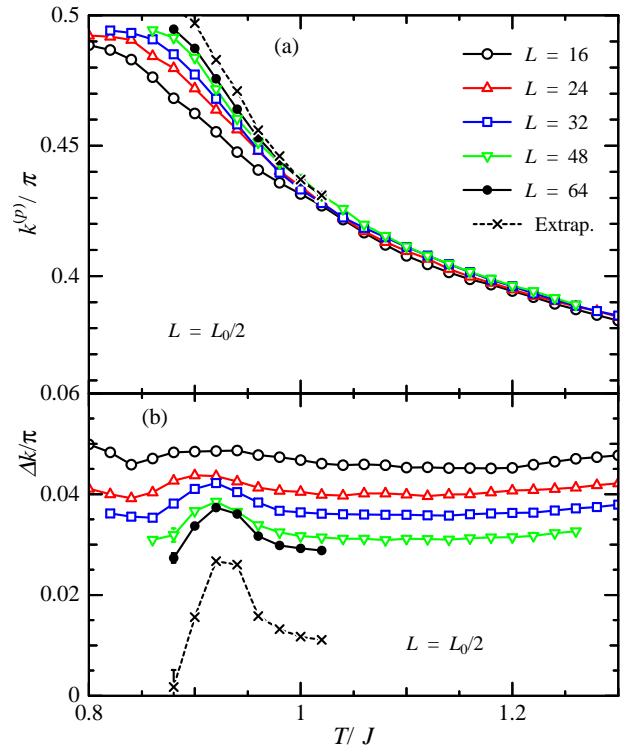


FIG. 8. (color online) Temperature dependences of $k^{(p)}$ and Δk of the lattice with L in the ANNNI model with $\kappa = 0.6$. The extrapolations to $L \rightarrow \infty$ for $k^{(p)}$ and Δk are made using $k_L^{(p)} = k_{\infty}^{(p)} + A/L$ and $\Delta k_L = \Delta k_{\infty} + B/\sqrt{L}$ assumptions, respectively.

functions of T , respectively, together with their extrapolated values. As the temperature is decreased from a high temperature, $k^{(p)}$ increases toward $k^{(p)} = \pi/2$ at T_{C2} . On the other hand, Δk changes a little above T_{C2} and the extrapolation value has a finite value, suggesting that some quasi-periodic spin structure occurs above T_{C2} . A notable thing is that Δk has a mound near above T_{C2} . Again we see that the diversity of the spin structure along the y -direction is enhanced at $T \gtrsim T_{C2}$. For $T < T_{C2}$, Δk diminishes revealing that the spin structure in the $\langle 2 \rangle$ phase is periodic with period four.

VI. DISCUSSION AND CONCLUSIONS

We have examined the spin ordering near the lower transition temperature T_{C2} of the 2D ANNNI model with $\kappa = 0.6$ having used a CHB Monte Carlo method. We considered an N_R -replica system and calculated an overlap function q_m between different replicas. We determined $T_{C2}/J = 0.89 \pm 0.01$ and examined the nature of the spin structure at $T \gtrsim T_{C2}$ by the use of different quantities. The results were summarized in Fig. 9.

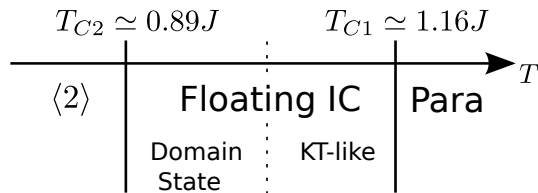


FIG. 9. (color online) The spin ordering of the 2D ANNNI model with $\kappa = 0.6$

In the floating IC phase, the nature of the spin correlation for $T \gtrsim T_{C2}$ are considerably different from that for $T \lesssim T_{C1}$. For $T \gtrsim T_{C2}$, the system is characterized by large domains each of which run across the lattice. Therefore we may call the spin structure for $T \gtrsim T_{C2}$ a domain state.

In the domain state in Fig. 9, the 2D XY symmetry of the spin correlation breaks, i.e., the spin correlation length in the axial direction ξ_y decreases with lowering temperature in contrast with a monotonous increase of that in the chain direction ξ_x . In consequence, the diversity of the spin arrangement increases as $T \rightarrow T_{C2}$ and the Binder ratio g_L exhibit a depression at $T \sim T_{C2}$. Also the quasi-periodic spin structure, which is realized in the IC phase, becomes diverse at $T \gtrsim T_{C2}$.

Here we consider properties of the domain state. We first note that an isolated domain is unstable, because it readily collapses with thermal noise. On the other hand, the domain state occurring at $T \gtrsim T_{C2}$ is sequentially arranged four types of domains: $A \rightarrow \bar{B} \rightarrow \bar{A} \rightarrow B \rightarrow A \rightarrow \bar{B} \dots$. This structure is stable against the thermal fluctuation. We consider the A -type $\langle 2 \rangle$ phase with three domains of \bar{B} , \bar{A} , and B . Suppose that the \bar{B} domain collapses. Then domain arrangement becomes as $A \rightarrow \bar{A} \rightarrow B \rightarrow A$ and an unfavorable domain wall of $W_{A-\bar{A}}$ appears. This domain structure is unstable and as soon as the \bar{B} collapses, another \bar{B} arises between the A and the \bar{A} domains, because further collapse of the \bar{A} also yields unfavorable domain wall W_{A-B} . Therefore the collapse of three domains of \bar{B} , \bar{A} , and B will occur concurrently. This is a very rare event especially at low temperatures, because the domain size becomes larger and larger as the temperature is decreased toward T_{C2} . The reverse is also true. That is, the concurrence of three domains in the $\langle 2 \rangle$ phase is also very rare event. These properties explain a well-known phenomenon of the 2D ANNNI model, i.e., a huge number of the MC sweep is necessary to get an equilibrium spin configuration.

Also development of the spin structure exhibits an interesting property in this temperature range. Figure 10 shows the development of the maximum spin overlap $q_m(t)$ starting with paramagnetic spin configuration for various temperatures. Here we adopt a single-spin-flip heat-bath MC algorithm and t being the number of the MC sweep. For a temperature well-above T_{C2} , $q_m(t)$ monotonously increases toward $q_m(\infty)$, which is estimated in the equilibrium CHB MC simulation. On

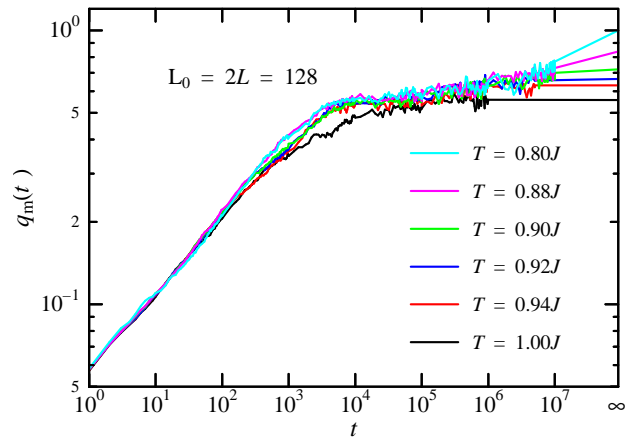


FIG. 10. (color online) The MC sweep t dependence of the maximum spin overlap $q_m(t)$ starting with paramagnetic spin configuration in the ANNNI model with $\kappa = 0.6$. The last points are ones estimated by the equilibrium CHB simulation.

the other hand, for temperatures $T \sim T_{C2}$, $q_m(t)$ exhibits two-stage development. In the first stage, it increases algebraically with t and reach a value of $q_m \sim 0.5$ at $\bar{t} \sim 10^4$, which are almost independent of the temperature (even for well-below T_{C2}). In the second stage, $q_m(t)$ slowly increases with t until $q_m(t)$ reaches its equilibrium value $q_m(\infty)$. Again we see $q_m(t)$ are almost independent of the temperature within this time scale. We find that this two-stage development of $q_m(t)$ comes from the domain structure of the model. Figure 11 shows the t dependence of $S(k)$ at $T \sim T_{C2}$. As t increases from $t = 0$, the peak of $S(k)$ develops and becomes of a single-peaked at $t \sim 10^4$. Above this time, the peak position k increases very slowly toward to k_p of the equilibrium result with clarifying its shape. That is, the first stage of the development of the spin structure is the creation of some quasi-periodic spin arrangement, and in the second stage the period of the periodic structure is gradually changes to fit its equilibrium one. The later stage is the collapse of different domains which is very slow as discussed above.

ACKNOWLEDGMENTS

We are thankful for the fruitful discussions with Professor S. Fujiki. Part of the results in this research was obtained using supercomputing resources at Cyberscience Center, Tohoku University.

REFERENCES

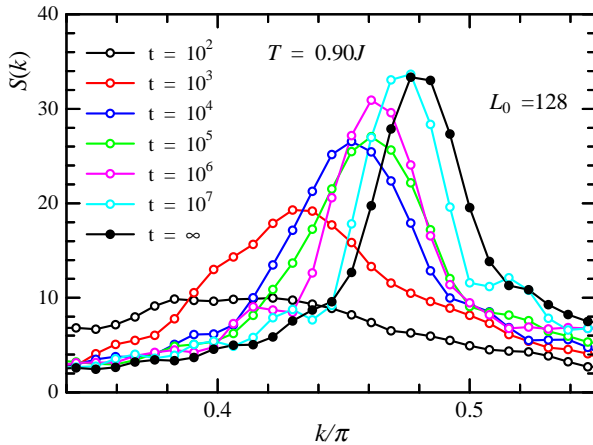


FIG. 11. (color online) The MC sweep t dependence of the Fourier component $S(k)$ of the spin structure starting with paramagnetic spin configuration in the ANNNI model with $\kappa = 0.6$. $S(k)$ for $t = \infty$ is one estimated by the equilibrium CHB simulation.

* shira@iwate-u.ac.jp

- ¹ For example see, e.g., W. Selke, in *PHASE TRANSITIONS AND CRITICAL PHENOMENA*, ed. C. Domb and J. L. Lebowitz (Academic Press, 1992), Vol. 15, p. 1; and references therein.
- ² W. Selke and M.E. Fisher, *Z. Physik B* **40**, 71 (1980).
- ³ W. Selke, K. Binder, and W. Kinzel, *Surf. Sci.* **125**, 74 (1983).
- ⁴ J. Villain and P. Bak, *J. Phys.(Paris)* **42**, 657 (1981).
- ⁵ M. D. Grynberg and H. Ceva, *Phys. Rev. B* **36**, 7091 (1987).
- ⁶ M. A. S. Saqi and D. S. McKenzie, *J. Phys. A: Math. Gen.* **20** 471 (1987).
- ⁷ Y. Murai, K. Tanaka and T. Morita, *Physica A* **217**, 214 (1995).
- ⁸ J. M. Kosterlitz and D. J. Thouless, *J. Phys. C* **6**, 1181 (1973).

- ⁹ A. Sato and F. Matsubara, *Phys. Rev. B* **60**, 10316 (1999).
- ¹⁰ E. Rastelli, S. Regina and A. Tassi, *Phys. Rev. B* **81**, 094425 (2010).
- ¹¹ N. Ito, *Physica A* **192**, 604 (1993).
- ¹² N. Ito and Y. Ozeki, *Int. J. Mod. Phys. C* **10**, 1495 (1999).
- ¹³ T. Shirahata and T. Nakamura, *Phys. Rev. B* **65**, 024402 (2001).
- ¹⁴ A. K. Chandra and S. Dasgupta, *J. Phys. A: Math. Theor.* **40** 6251 (2007).
- ¹⁵ T. Shirakura, F. Matsubara, and N. Suzuki, *Phys. Rev. B* **90**, 144410 (2014).
- ¹⁶ O. Koseki and F. Matsubara, *J. Phys. Soc. Jpn.* **66**, 322 (1997).
- ¹⁷ F. Matsubara, A. Sato, O. Koseki, and T. Shirakura, *Phys. Rev. Lett.* **78**, 3237 (1997).
- ¹⁸ K. Binder, *Z. Phys. B: Condens. Matter* **43**, 119 (1981).
- ¹⁹ F. Cooper, B. Freedman, and D. Preston, *Nucl. Phys. B* **210**, 210 (1989).